



ELSEVIER

Nuclear Instruments and Methods in Physics Research A 474 (2001) 38–45

**NUCLEAR  
INSTRUMENTS  
& METHODS  
IN PHYSICS  
RESEARCH**  
Section A

www.elsevier.com/locate/nima

# Array of scintillator counters for PHOBOS at RHIC

R. Bindel<sup>a</sup>, E. Garcia<sup>a,\*</sup>,<sup>1</sup>, A.C. Mignerey<sup>a</sup>, L.P. Remsberg<sup>b</sup>

<sup>a</sup>University of Maryland, College Park, MD 20742, USA

<sup>b</sup>Brookhaven National Laboratory, Upton, NY 11973, USA

Received 6 February 2001; accepted 10 February 2001

---

## Abstract

An array of scintillator counters (“paddle counters”) for the measurement of number and energy of charged particles in heavy-ion gold–gold collisions for the PHOBOS experiment at RHIC is described. These simple, versatile, and highly efficient detectors provide a low bias and an easily understood level zero trigger. The paddle counters can also be used to select and measure event centrality. The information from the paddle counters used for triggering and event selection included the total signal height (proportional to the number of particles), the timing information of the hits, and the number of scintillators fired. The general characteristics of the paddle counters, their design parameters, and performance during the first run at RHIC are presented in this paper. © 2001 Elsevier Science B.V. All rights reserved.

PACS: 29.40.Mc; 29.90.Tr

Keywords: Scintillator; Trigger; Paddle

---

## 1. Introduction

The Relativistic Heavy Ion Collider (RHIC) at Brookhaven National Laboratory has delivered the first collisions between Au nuclei at the highest center-of-mass energies achieved in the laboratory to date. PHOBOS, one of the four RHIC experiments, is designed to track charged particles in a magnetic field, determine the interaction vertex, and measure the multiplicity of charged particles produced in heavy-ion gold–gold collisions. The experiment consists of several sub-

systems: single-layer Si pad multiplicity detectors, two Si spectrometer arms utilizing planes of silicon pad and strip detectors, two time-of-flight walls, two zero degree calorimeters, and the trigger detectors. A complete description of the experimental layout can be found in Ref. [1]. The present paper provides a detailed description of the primary trigger detectors, the paddle counters.

The run strategy of PHOBOS for the first few years of RHIC running was to examine these collisions in as unbiased a way as possible. With this in mind, the paddle counters, the primary trigger detectors, were built to handle a broad range of experimental conditions. Plastic scintillators are ideal for this purpose, since they allow a large dynamic detection range (from one to 50 minimum ionizing particles (mips) per interaction in the present application), do not require

---

\*Corresponding author. Tel.: +1-631-344-3983; fax: +1-631-344-1334.

E-mail address: edmund.garcia@bnl.gov (E. Garcia).

<sup>1</sup>Brookhaven National Laboratory, Physics 510D, Upton, NY-11973, USA.

complicated readout electronics (cost effective), and are able to withstand large doses of radiation. The main characteristics that distinguish the paddle counters are: their high triggering efficiency (100% for central and semi-peripheral Au–Au collisions), allowing a minimum bias selection of events; their ability to discriminate events with different multiplicities, permitting clear rejection of background; and the use of energy deposition as a means to measure the relative centrality of the collisions. Finally, the simplicity of the geometry and the design, based on a modular scintillator-phototube array, makes these detectors relatively easy to simulate and understand.

The paddle counters were designed in a modular fashion. This modularity allowed two distinct means of triggering and event selection, one based on the number of modules hit in each interaction and the other based on the individual module pulse height and timing information. Used in conjunction, this information provides a proportional measurement of the number of charged particles hitting the detector, and a means by which to select the event centrality.

## 2. Geometry and design characteristics

The paddle counters are two sets of 16 scintillators located at  $-3.21$  m (PN) and  $+3.21$  m (PP) from the nominal interaction point along the beam axis ( $z$ ). The scintillators form disks perpendicular to the  $z$ -axis that encircle the beam line. The paddle's active area subtends 99% of the solid angle over a range of  $3 < |\eta| < 4.5$  in pseudo-rapidity units. The beam pipe is a Be tube of 5-cm exterior radius; the distance between the tip of the scintillator and the beam pipe is 2 cm. Fig. 1 is a diagram of a complete paddle counter and Fig. 2 shows the elements of one of the unit modules, where (a) is the scintillator, (b) is the magnetic shield, (c) is the phototube, and (d) is the light guide.

The individual scintillators are made of BC-400 plastic and are 18.6 cm in length, 0.95-cm thick, and 1.9-cm long at the inner edge and 9.5-cm long at the outer edge. The light guide (BC-800) has two components, one that couples with the scintillator

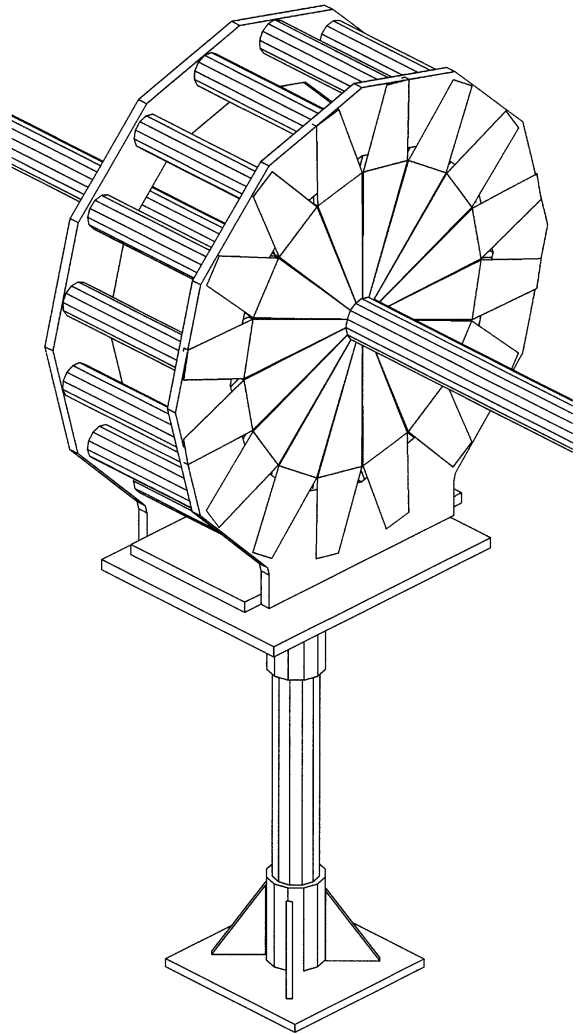


Fig. 1. Diagram of a paddle counter and a section of the Be beam pipe.

and another that couples with the phototube. A  $45^\circ$  aluminized mirror reflects the light through the  $90^\circ$  angle between the two components of the light guide. The scintillator and the light guide are coupled with BC-500 optical epoxy. At the end of the light guide, a hybrid photomultiplier tube assembly, H1151-2 from Hamamatsu, is attached with silicon elastomer. Surrounding the tube, and attached to the light guide, is a 2-mm mu-metal magnetic shield. The tube inside the magnetic shield is made light tight with black epoxy, while

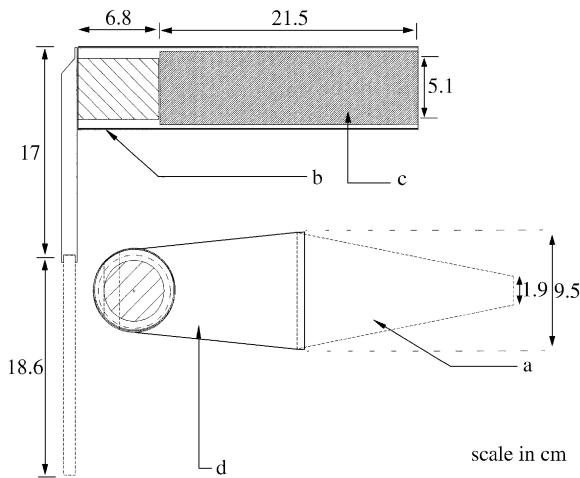


Fig. 2. The elements of one of the unit modules of the paddle counters: the scintillator (a), the magnetic shield (b), the phototube (c), and the light guide (d).

the light guide and scintillator are wrapped with a layer of aluminum and a layer of black vinyl.

The mechanical structures that hold the modules are made of glass reinforced Ultem; they were designed and built by the Electronics and Development Group of the University of Maryland. The scintillator, light-guide, phototube modules were designed by the University of Maryland in cooperation with BICRON. The modules were assembled by BICRON.

An important characteristic of the design of the paddle counters is that the detectors are not sensitive to the direction of the beam. That is, there is no difference in the module response to the particles hitting from the front or from the back of the scintillator. This becomes relevant for beam background studies, as explained later in this paper.

### 3. Response and calibration

During the RHIC running periods it is expected that each paddle detector will give a common response to a given event; thus, it was necessary to study the individual module response and then match the gain and the timing of every module. Fig. 3 is a plot of the normalized mean of the pulse

height distributions ( $\Delta E$ ) measured in one module from a collimated source of minimum ionizing particles (mips) as a function of the position on the scintillator. The shape in the figure is the actual geometry of the face of the scintillator. The pulse height readings were measured with an analog to the digital converter (ADC); the readings were done for every square centimeter using a collimated  $^{106}\text{Ru}$  source of 3.5 MeV beta particles. The trigger condition was established with the coincidence of the paddle's scintillator and a second smaller (1 cm  $\times$  1 cm) scintillator. Fig. 3 shows the normalized mean of the pulse height distributions measured at each point, in a lego surface and in a contour representation. Each point is normalized to the highest value found in the mapping. Similarly, Fig. 4 shows the relative time response of the paddle's scintillator. At each point on the face of the scintillator, the start for the time to digital converter (TDC) was given by the small scintillator (in coincidence with the paddle), while the stop was given by the arrival time of the signal from the paddle. The  $\Delta T$  plotted is the difference in the mean of the time distributions at each point minus the lowest mean found in the mapping.

The highest  $\Delta E$  values of the mapping are found at the small (inner) edge of the scintillator, with the  $\Delta E$  decreasing gradually as the position of the readings moves closer to the light guide. Nearest to the light guide ( $y = 0$  in Fig. 3),  $\Delta E$  is about 45% lower than the maximum value. The horizontal ( $x$ ) variation of  $\Delta E$  is small, but  $\Delta E$  is higher when the readings are closer to the edge of the scintillator for some vertical ( $y$ ) slices. Assuming the ionization energy from one minimum ionizing particle hitting perpendicularly to the face of the scintillator at any position ( $x, y$ ) is constant, the variations of the pulse height must be related to the different paths that the light takes through the scintillator. From a given ionization point, the light expands radially; part of the light flux will go directly to the light guide while part of it will hit the edges of the scintillator and be reflected, finding its way to the light guide at a later time. Each time the light hits an edge, part of it escapes from the scintillator. Given the geometry, chances are that the light flux from an ionization point closer to the tip takes a more direct path towards the light guide; thus, the

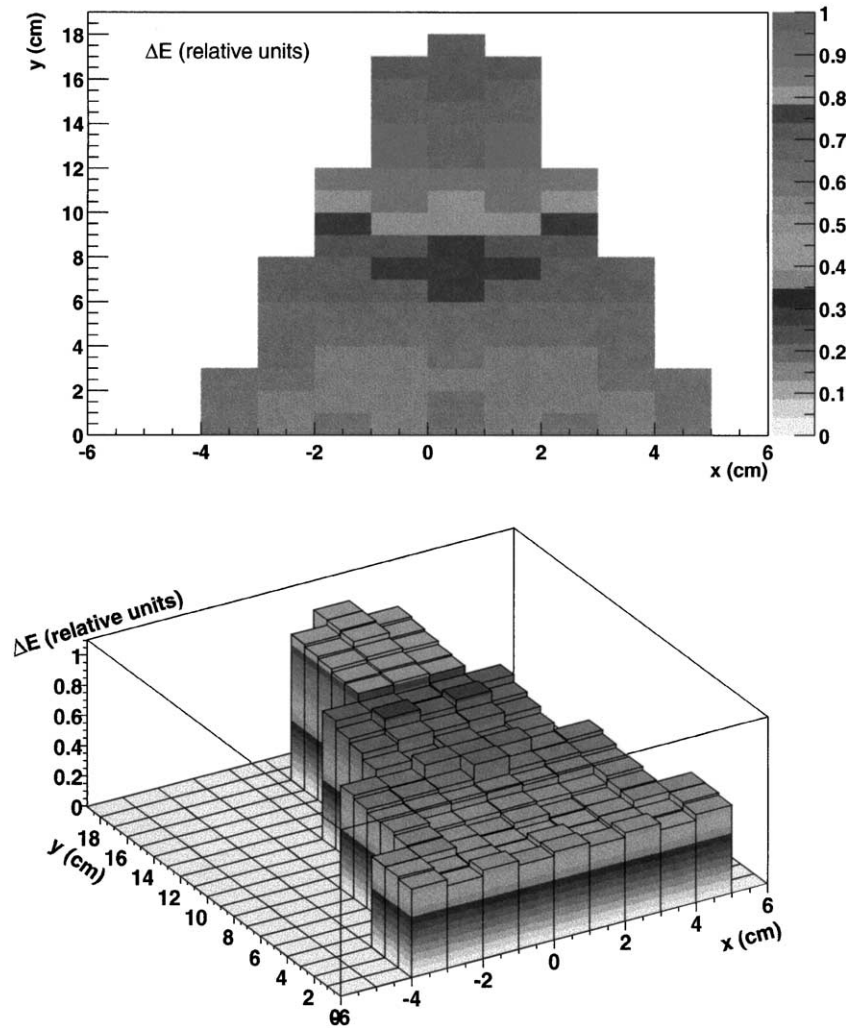


Fig. 3. Normalized mean ( $\Delta E$ ) of the distribution of the energy deposited in one module from a collimated source of minimum ionizing particles, as a function of the position on the face of the scintillator.

$\Delta E$  is higher, and the opposite is true for the points closer to the light guide. Finally, it was found that the energy resolution ( $\sigma_E/\Delta E$ ) remains approximately constant over the face of the scintillator, varying only from 11% to 14%.

On the other hand, as expected, the lowest values of relative time response ( $\Delta T$ ) are from points closer to the light guide, since the leading edge of the light pulse travels less distance from those points to the tube. The time resolution  $\sigma_T$  over the face of the scintillator is quite constant,

with a few fluctuations between 300 and 400 ps. Note that this is an upper limit to the intrinsic resolution since it has the small scintillator resolution (about 150 ps) folded in.

The relative calibration of the 16 modules for each paddle was done in two parts. First, a calibration was done using a radioactive source prior to the experimental run. Subsequently, a more refined calibration was done with beam interactions during normal RHIC operation. For the source calibration, a pulse height and time

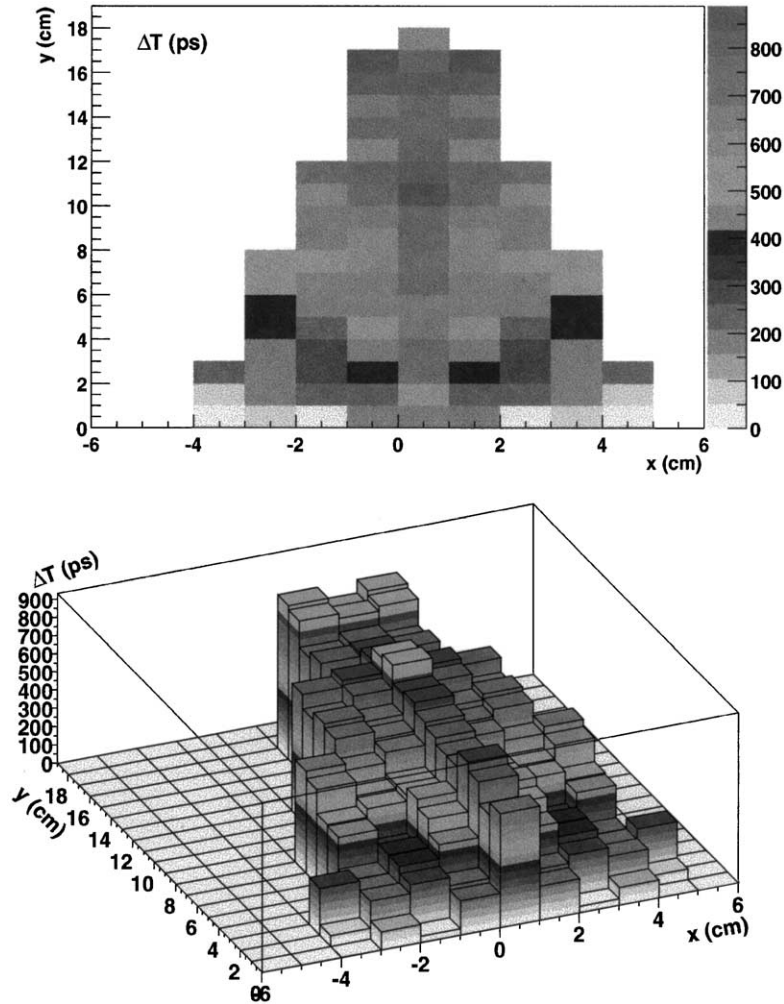


Fig. 4. Relative mean ( $\Delta T$ ) of the time distribution of the response of one module to the minimum ionizing particles as a function of the position on the face of the scintillator.

response point were taken for every module at three different voltage settings. The position of the calibration points on the scintillator face was in the center ( $x = 0$ ), about 15 cm from the light guide in  $y$ . Using the pulse height and the relative time difference of the calibration points, a gain curve and a delay curve were established for each module. The gains of each set of 16 modules in each paddle were then matched and the relative time delay from the intrinsic response was corrected with delay cables.

The second part of the calibration took place with the beams circulating in the machine and the detectors in running position. Looking at the one mip peak from the beam interactions, the gains were refined. The relative time delays among the modules of each detector were corrected with delay cables. At this stage of the calibration, the relative delay included the time mismatches of the signal cables and electronics. Fig. 5 is the spectrum of the sum of the ADC signals from all the modules of the negative paddle counter from a typical run.

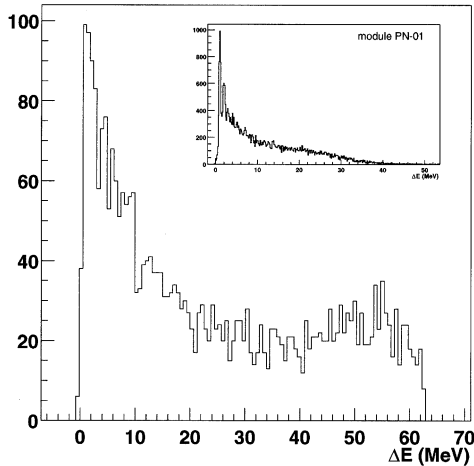


Fig. 5. The spectrum of the sum of the ADC signals from all the modules of the negative paddle counter from a typical run. The ADC spectra are calibrated to the energy deposited by one mip in the scintillator. The inset is the single ADC spectrum for one of the modules of the negative paddle counter.

Negative and positive were the terms given to the paddle counters on either sides of the interaction region. As a reference, an inset is included in the figure which shows the ADC spectrum for only one of the modules; this clearly shows the one, two, and three mip peaks. The ADC spectrum is calibrated to the energy deposited by one mip in the scintillator ( $\Delta E = 1.7$ ) in MeV. The signal-to-noise ratio for the paddle counters was found to be about 20:1. The one mip resolution was about  $\sigma_E/\Delta E = 45\%$ . This resolution is not much larger than the resolution found for the individual ADC signals of each module during the bench test. The 45% is consistent with the variations in the amount of light collected from different points in the scintillator.

Fig. 6 is the distribution of the time difference between the positive and negative hard sums of the paddle signals, for minimum bias Au + Au collisions. The hard sum for the positive and negative paddles is the sum of the currents from each of the 16 tubes. The time resolution was about  $\sigma_T = 1.0$  ns, not much larger than the time resolution found during the calibration with the source, if we take into account that the particles can hit any point on the face of the scintillators.

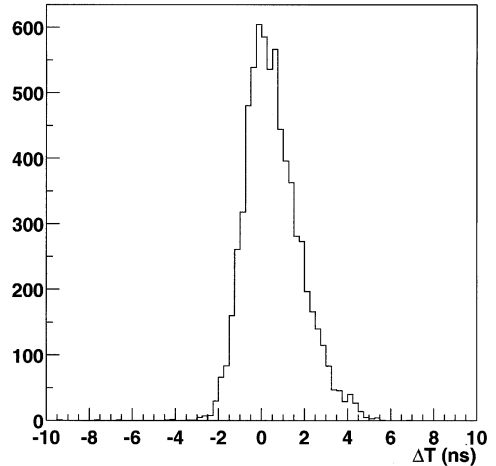


Fig. 6. The distribution of the time difference between the positive and negative hard sums of the paddles for minimum bias, central Au + Au collisions.

This demonstrates the good time matching of individual paddle modules.

#### 4. Run performance

The minimum bias trigger used in PHOBOS during the summer 2000 run selected events based on the coincidence of at least one hit in any of the modules of both the positive (PP) and negative (PN) paddles, within a time window of 76 ns (the PP and PN gates were set at 38 ns each). This trigger selected collision events as well as various forms of background. The background rejection was then achieved either through hardware (on line) or software (off line). This depended on the machine conditions, the physics analysis and the capabilities of the data acquisition system at different points during the run.

The first condition for background rejection is a requirement that the paddle time difference be less than 76 ns between the PP and PN signals, eliminating the background that was not synchronized (within that time window) with the beams crossing. Another background cut is achieved by the requirement that more than one module of each paddle counter be hit in coincidence; that is, it requires a coincidence between  $PP(n)$  and  $PN(n)$ ,

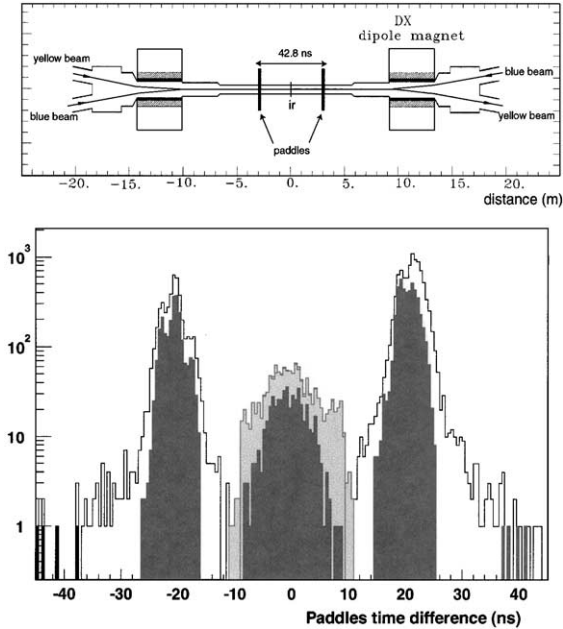


Fig. 7. The distribution of the time difference between the positive and negative paddles for different trigger conditions from Au + Au at  $\sqrt{s} = 130$  A GeV. The distribution with white background is the minimum bias trigger distribution. Shown in gray is the occupancy trigger selection  $PP(n)$   $n > 3$  and  $PN(n)$   $n > 3$ , and in dark gray is the distribution resulting from a cut in the time difference of 11 ns.

where  $n$  is the number of modules that have fired in a given paddle counter. Finally, the sum of the currents from the pulses of each of the 16 modules in a paddle can be discriminated at a certain level to produce the logic signals  $PP_{\text{sum}}$  and  $PN_{\text{sum}}$ , which on coincidence gives a centrality trigger.

Fig. 7 shows the distribution of the time difference between the positive and negative paddles from Au + Au at  $\sqrt{s} = 130$  A GeV for different trigger conditions. The distribution with a white background is the minimum bias distribution, triggered with the condition of a coincidence between the 38-ns PP and PN gates. This distribution includes both the background and collision events (e.g. beam gas events or scattering upstream and downstream of the detectors). Shown in gray is the occupancy trigger selection  $PP(n)$  and  $PN(n)$ ,  $n > 3$ . After applying this condition, three regions are observed in the spectra; the central corresponding to collisions

and double beam background, and the other two, centered at  $\pm 22$  ns, which are mostly due to the beam gas interactions and/or beam halo. This is represented graphically in the diagram on the top of Fig. 7. The beam circulating clockwise has been named “yellow” by the RHIC operators, while the beam circulating counterclockwise is “blue”. For the single beam background events, an interaction is produced either by the yellow or, in the opposite direction, by the blue beam. The interaction particles will hit one of the paddles in the back and then, 44 ns later, the other in the front. It was not possible to distinguish between collisions and double beam events, since both give the same time information in the paddles. However, by using experimental runs where the beams did not collide, it was found that the overall rate for the double beam background was less than 1% for all events. Finally, the dark gray spectrum in Fig. 7 shows the events triggered with a 11-ns coincidence gate.

The paddles proved to be good tools to calculate the event centrality for physics analysis. The assumption underlying this statement is that the number of particles hitting the paddle counters in a collision increases monotonically with the increasing number of participants, which is a measure of the reaction centrality. As explained in detail in Ref. [2], in order to select the 6% most central events, the mean of the normalized ADC values of the individual modules of each of the paddles was used. On an average, one mip from the collision will deposit about 1.7 MeV in the scintillators. Fluctuations to this energy may occur due to slow secondary particles that traverse the counters at large angles. To reduce this effect, instead of the average of the 16 modules, only the average pulse height of the 12 lowest signals from the 16 scintillators of each paddle was used to calculate the signal sums ( $PN_{12}$  and  $PP_{12}$ ). Then, the mean paddle sum  $\frac{1}{2}(PN_{12} + PP_{12})$  was used as an observable proportional to the number of particles detected by the paddles, the largest 6% of events in this sum representing the 6% most central events of all collisions. These events were used to extract the charged particle multiplicity from the silicon to the number of particles detected by the paddles, with the largest 6% of events in this sum representing the 6% most central events

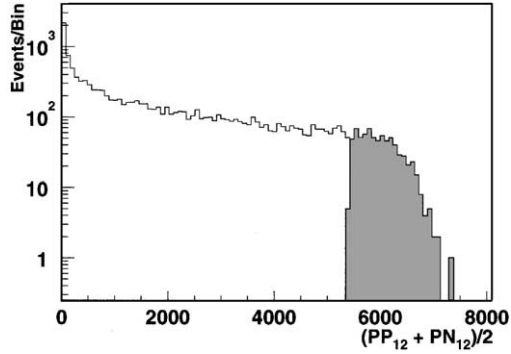


Fig. 8. Paddle sum signal distribution for events at  $\sqrt{s} = 130$  A GeV. The shaded region corresponds to the spectrum obtained with the centrality cut at 6% of events with the largest mean paddle sum.

of the collision. These were the events used to extract the charged particle multiplicity from the silicon detectors. Fig. 8 shows the derived sum of the paddle signal distribution for events at  $\sqrt{s} = 130$  A GeV. The centrality cut at 6% of events with the largest mean paddle sum is shown as the shaded region.

## 5. Final notes

During the first physics run of RHIC, the paddle counters achieved a signal-to-noise ratio of 20 : 1, with a time resolution of about 1 ns. The paddle counters provided an effective minimum bias trigger and were able to effectively discriminate Au + Au collisions from the machine background.

The combination of total signal height (proportional to the number of particles detected), the number of modules fired, and the time distribution of the hits provided a means to create a selective off-line event trigger. Furthermore, the total energy deposited in the paddles was used to select the event centrality, which proved to be very important for the publication of the first PHOBOS result [2]. The paddle counters should be useful when RHIC runs different ion species, as well as for the p + A, and p + p future runs.

## Acknowledgements

We would like to thank all those who helped in the design and construction of the paddle counters: Richard Baum and the Electronics and Development Group of the University of Maryland who designed and supervised the construction of the mechanical structures; Sean McGuinnis and Bicon Corporation, who cooperated in the designing of the light guides and supervised the assembly of the modules. Finally, we acknowledge the effort of all the members of the PHOBOS collaboration. This research has been supported by the US Department of Energy under the grant DE-FG02-93ER40802.

## References

- [1] PHOBOS conceptual design report, BNL 1994.
- [2] B. Back, et al., Phys. Rev. Lett. 85 (2000) 3100.